PARIS

Process Attribution of Regional Emissions

GA 101081430, RIA

Complete calendar year of extended and quality controlled CH_4 data uploaded to the ICOS portal, included in D4.3

M39			
Delivery due date Annex I	01/05/2025		
Actual date of submission	20/02/2026		
Lead beneficiary: EMPA	Work package: 5	Nature: Report/data	Dissemination level: Public
Responsible scientist	Tim Arnold		
Contributors	Stephan Henne EMPA, Anita Ganesan UNIVBRIS, Alistair Manning MO, Tim Arnold (UNIEDIN)		
Internal reviewers			
Version: 1.1			

Horizon Europe Cluster 5: Climate, energy and mobility

"This project has received funding from the European Union's Horizon Europe Research and Innovation programme under HORIZON-CL5-2022-D1-02 Grant Agreement No 101081430 - PARIS".

Table of content

1. Changes with respect to the DoA (Description of the Action)

Although the report and associated data upload were delayed beyond the original timeline, the contents of the deliverables and milestone outcomes are unchanged from the DoA.

2. Dissemination and uptake

The data collected/produced as part of this milestone are relevant for the production of the Annex reports in WP2. As such they have been shared with the relevant project partners prior to the completion of D4.3 and D2.3. Final data products are all available publicly on the ICOS Carbon Portal for use by other scientists and practitioners.

3. Short Summary of results

The ICOS ATC collection of European methane (ObsPack Europe, https://meta.icos-cp.eu/objects/Cogv2ldYfPN0OgVTRecFgzab) was used as input to the inversion modelling systems employed in PARIS, combining a total of six combinations of inversion systems (RHIME, InTEM, ELRIS) and transport models (NAME, FLEXPART). Inverse modelling results include monthly CH_4 fluxes at a spatial resolution of 25 km x 25 km and country aggregates for the European domain. These were collected in commonly defined data formats and made publicly available (https://doi.org/10.18160/GR1Q-6SK4).

4. Evidence of accomplishment

Inverse modelling results (including flux estimates as well as observed and simulated atmospheric mole fractions) from the individual inversions are available on the ICOS Carbon Portal:

ELRIS-FLEXPART, https://meta.icos-cp.eu/objects/od9o-Uka9A0b1lV-Z0lk-WeF

ELRIS-NAME, https://meta.icos-cp.eu/objects/gp1oRDdSjjeWRC805PY6-zFH

InTEM-FLEXPART, https://meta.icos-cp.eu/objects/5W5IE8X5xTyslvq_FjrRv-kV

InTEM-NAME, https://meta.icos-cp.eu/objects/TFCu1I52WEBjnW_2jwaDhb0o

RHIME-FLEXPART, https://meta.icos-cp.eu/objects/b4lh_958ogPzX70cv-YrvZ4Y

RHIME-NAME, https://meta.icos-cp.eu/objects/XIH2WO6haVE3HdoRvApr_5yy

4.1 Introduction | Background of the deliverable | milestone

Observations of greenhouse gases form the backbone of any inverse estimate of greenhouse gas fluxes to the atmosphere. Inverse estimates of CH_4 were made using the described atmospheric measurements of mole fractions. Use of atmospheric transport models is necessary to translate these atmospheric measurements into estimates of emissions from the surface. Multiple methods and analyses can be used to couple models with atmospheric data, which can vary significantly, for example through the data filtering methodologies, resolution of the transport model output, transport model setup, and execution of the statistical inversion technique. Team members have each published their own independent methods and results on the use of their inversion systems in estimating greenhouse gas emissions (e.g., Manning et al., 2021; Redington et al., 2023; Katharopoulos et al., 2023; Henne et al., 2016; Ganesan et al., 2015, Lunt et al., 2021). A detailed common description of the inversion systems and their specific setup for PARIS was compiled as an annex to PARIS deliverable D2.3. Throughout the project, CH_4 emissions estimates will be derived for Europe across a matrix of transport models and inversion setups through this project, using new observations collected in the project (University of Bristol: RHIME-NAME, RHIME-FLEXPART; Met Office: InTEM-NAME InTEM-FLEXPART; EMPA: ELRIS-NAME and ELRIS-FLEXPART).

4.2 Scope of the deliverable | milestone

This milestone forms the basis for the inverse modelling results that form deliverable D4.3 and are in turn used in the draft Annexes provided to the national inventory teams for their 2026 reporting to the UNFCCC (D2.3).

4.3 Content of the deliverable | milestone

4.3.1 Overview

This report covers a description of the applied inversion systems and their performance evaluation against observations. The results of the inversions (monthly CH_4 fluxes for the period 2016 to 2024) are discussed in deliverable D4.3.

4.3.2 Observations and network sensitivity

Fig. 1 gives an overview of all CH_4 observations available for and used by the different inversion systems. 40 sites are listed in the figure, and all the displayed data were used in the inversions. Next to mole fraction, the observational data also contains estimates of measurement uncertainty (understood as the repeatability of a mole fraction observation, estimated from target gas measurements) and the sub-hourly variability of the observations. The latter is used by the inversion systems as a proxy for model uncertainty as situations with large observed mole fraction variability are considered to align with situations in which the models have difficulties reflecting these variabilities and, consequently, also the mean.

The combined 'coverage' of the CH_4 observations is depicted in Fig. 2 as the simulated (transport model FLEXPART) average source sensitivity for the year 2018 and 2024.

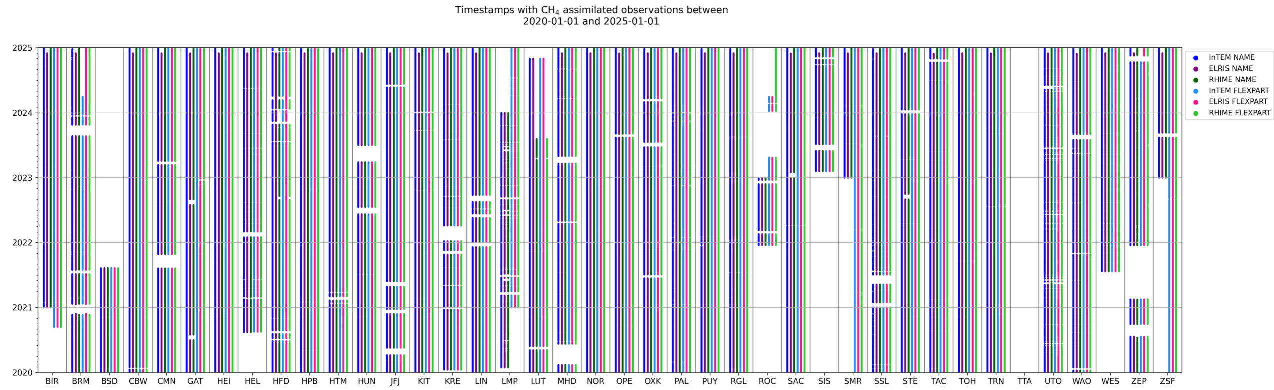

Fig. 1: CH_4 observational data usage by the different employed inversion models for the period 2020 to 2024. Note that some sites did not report any data during this period (but previously), whereas other sites stopped reporting.

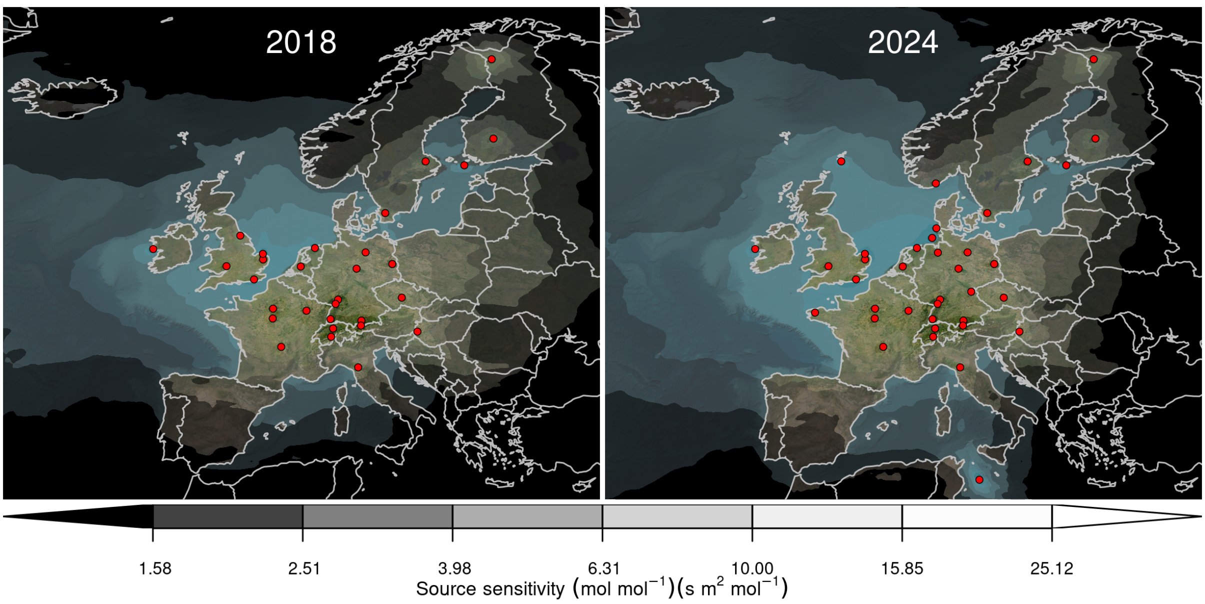

Fig. 2: Average monthly total source sensitivity of CH4 observing sites as calculated by the FLEXPART transport model for the year 2018 (left) and 2024 (right) and used in the inversions. Observing stations active in each year are marked with red dots. Areas with visible land surface represent regions for which emissions can be observed well from the network. Shaded or dark areas represent regions for which limited emission information can be obtained from the network.

4.3.3 Inversion setup

A detailed description of the inverse model setup for the PARIS CH_4 inversions is provided as part of deliverable D2.3 and serves as documentation for the inventory teams. It includes both a comprehensive discussion of the employed inversion techniques as well as the specific settings used for the CH_4 inversions.

In short, all three inversion systems (RHIME, InTEM, ELRIS) can be run with source sensitivities calculated by the atmospheric transport models FLEXPART or NAME. A common data format for the source sensitivities allows flexible exchange of one transport with the other. All three inversion systems have in common that the state vector, which is optimised as part of the inversion, contains emission and baseline elements. In all systems, a spatial aggregation of the emissions to larger areas (basis functions) is undertaken, but the details differ in terms of structure and number of state vector elements between the different systems. The baseline is treated by estimating the mole fractions at eleven interfaces around the common transport domain. The sensitivity of an observation to a baseline interface differs with time and is determined by the transport models as well. Common prior emissions are employed in all three models based on EDGAR 8.0 CH_4 emissions and the WETCHARTS wetland product. However, each modelling group made their own choices in terms of prior uncertainty and covariance structure. Mostly the same observations were used by all inversion systems (compare Fig. 1), but somewhat different filtering strategies, to avoid times with large model uncertainty, were employed. Different strategies were employed to determine the so-called model data mismatch uncertainty. Commonly, different sources of uncertainty (instrumental, model, baseline) were considered, but details differ between the systems.

4.3.4 Inversion performance analysis

An example CH_4 time series as observed and simulated at the site Beromünster (Switzerland, BRM), is given in Fig. 3. For each model system the figure shows the observations, the prior simulated mole fractions and the simulated mole fractions after emission optimisation (posterior simulation). Although the prior simulated time series already follows the observed time series well, the match is improved after optimisation as can also be seen in a reduced bias and RMSE as indicated in the histograms on the right. As seen above, the site is characterised by sharp pollution peaks in the summer months. These are only partly picked up by the simulations, which could indicate larger local to regional sources than estimated in the posterior.

Similarly, performance parameters were calculated for all sites and all model systems (Fig. 4). In most cases, posterior Pearson correlation coefficients were larger than 0.8, with only very few exceptions with correlation coefficients smaller than 0.6 being observed. No systematic difference in terms of performance can be discerned for different inversion systems and utilised transport models. The mean posterior bias was below 5 ppb in most cases. Centered RMSE were largely below 25 ppb, exceptions being the sites in the Netherlands (LUT and CBW) where CH_4 mole fractions tend to be the largest across the European network.

The Taylor plots in Fig. 5 serve as additional evidence of how comparison statistics were improved through the inversion. In this plot, posterior values generally are located closer to the expectation of a perfect model (correlation coefficient and normalized standard deviation of one) than their prior companions. Improvements for individual sites differ from model to model, but the general trend is the same for all inversions.

Although time series performance statistics are not an unambiguous proof that the obtained inversion results are close to the unknown true state, they still serve as an important indicator for an accurate setup and successful application of the inversion systems.

Fig. 3: Observed (black dots) and simulated (lighter colors prior, darker colors posterior) CH4 mole fractions at the site Beromünster (BRM) at the Irish west coast. Each sub-panel represents the comparison to one of the six inversion runs. The error bars give the model data mismatch uncertainty assumed by each model. The histograms

on the right give the prior (lighter) and posterior (darker) model-observation residuals, with μ and σ representing the mean bias an RMSE, respectively.

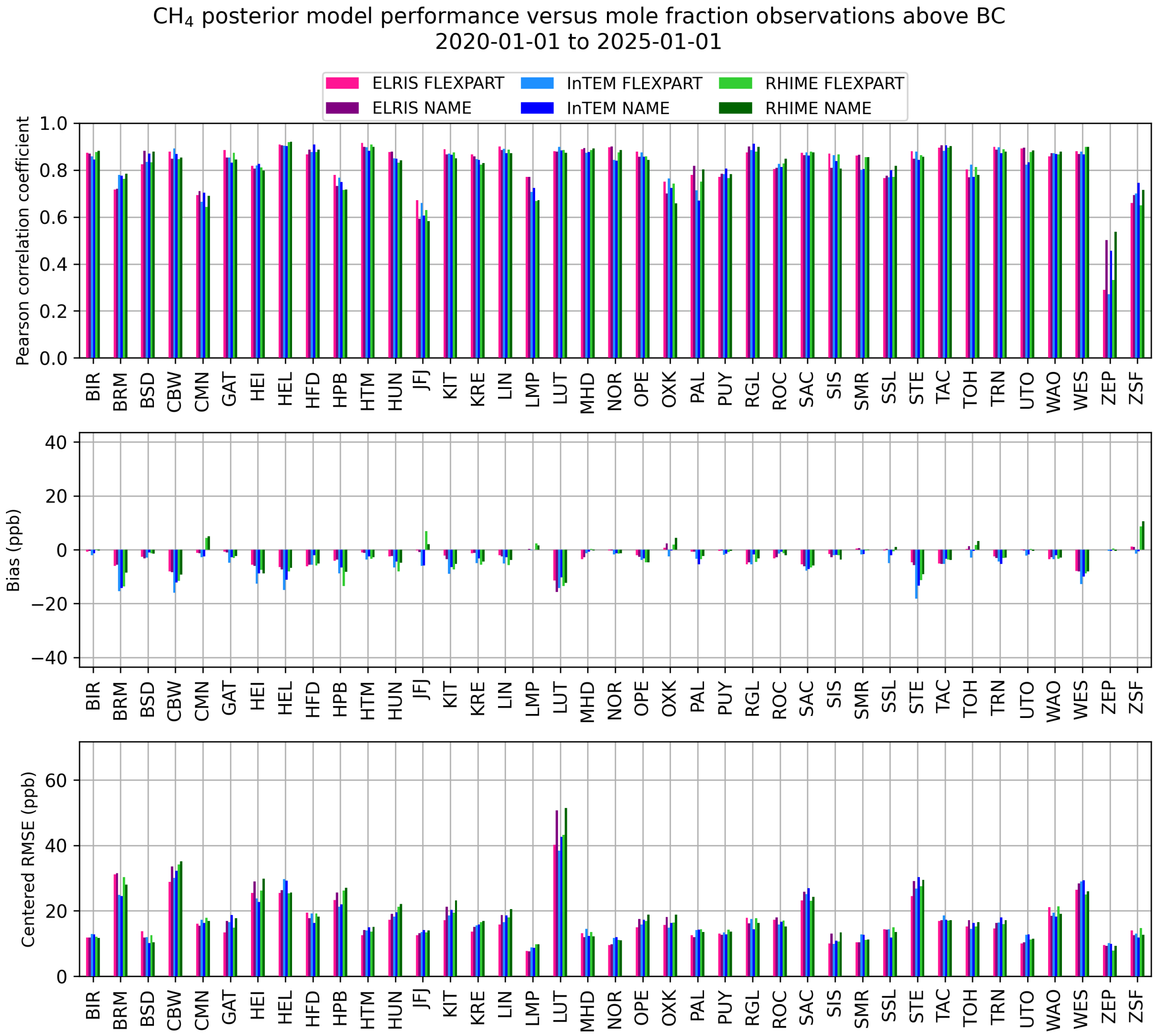

Fig. 4: Posterior model performance characterised by Pearson correlation coefficients (top), mean bias (middle), and centered RMSE (bottom) between observed simulated mole fractions above the baseline for all sites assimilated in the inversion and all model systems. Performance parameters were calculated for all observations in the period 2020 to 2024.

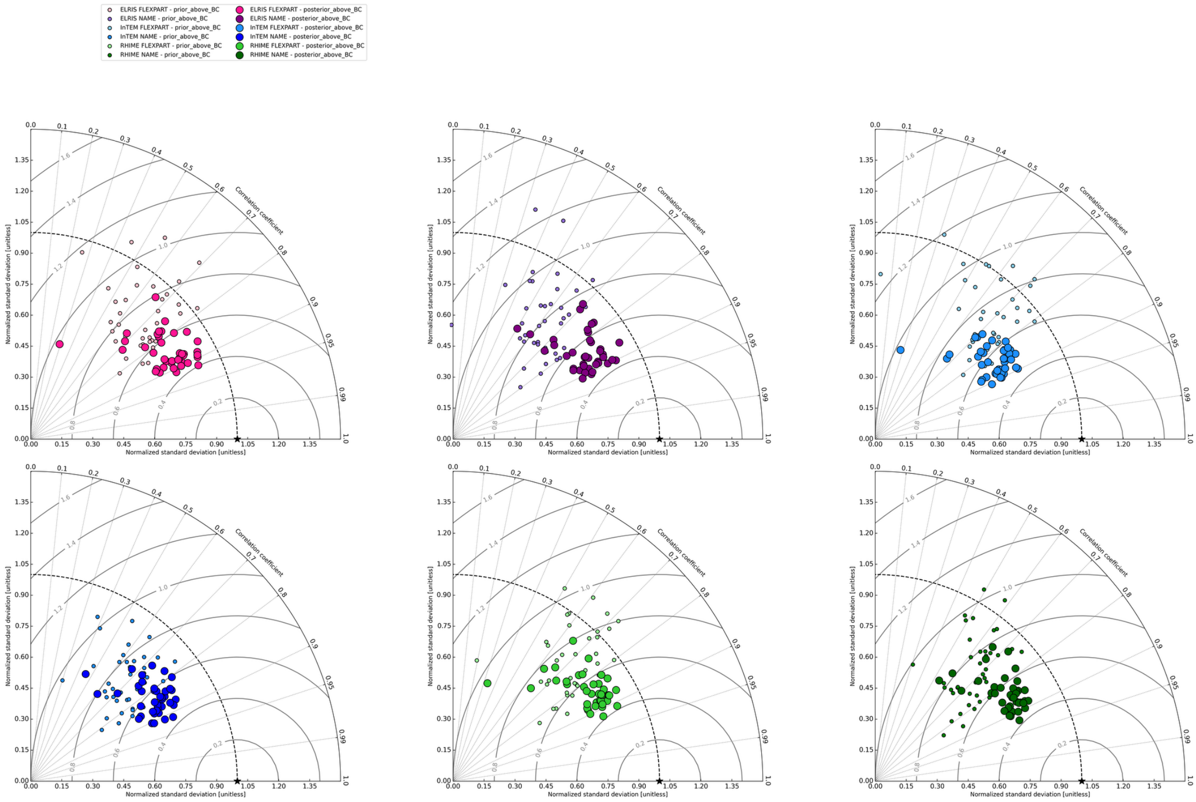

Fig. 5: Taylor plot of prior (small dots) and posterior (large dots) simulated posterior above-baseline mole fractions for the period 2020 to 2024 and separate for each model system.

4.4 Conclusion and possible impact

The set up and successful application of six inverse modelling systems allows for a robust estimation of CH_4 fluxes in north-western Europe. Fluxes will be reported as part of PARIS deliverable D4.3 and conclusions on the country level are reported to the respective national inventory teams as part of PARIS deliverable D2.3.

4.5 References

Ganesan, A. L., Manning, A. J., Grant, A., Young, D., Oram, D. E., Sturges, W. T., Moncrieff, J. B., and O'Doherty, S.: Quantifying methane and nitrous oxide emissions from the UK and Ireland using a national-scale monitoring network, Atmos. Chem. Phys., 15, 6393-6406, doi: 10.5194/acp-15-6393-2015, 2015.

Henne, S., Brunner, D., Oney, B., Leuenberger, M., Eugster, W., Bamberger, I., Meinhardt, F., Steinbacher, M., and Emmenegger, L.: Validation of the Swiss methane emission inventory by atmospheric observations and inverse modelling, Atmos. Chem. Phys., 16, 3683-3710, doi: 10.5194/acp-16-3683-2016, 2016.

Katharopoulos, I., Rust, D., Vollmer, M. K., Brunner, D., Reimann, S., O'Doherty, S. J., Young, D., Stanley, K. M., Schuck, T., Arduini, J., Emmenegger, L., and Henne, S.: Impact of transport model resolution and a priori assumptions on inverse modeling of Swiss F-gas emissions, Atmos. Chem. Phys., 23, 14159‑14186, doi: 10.5194/acp-23-14159-2023, 2023.

Lunt, M. F., Manning, A. J., Allen, G., Arnold, T., Bauguitte, S. J.-B., Boesch, H., Ganesan, A. L., Grant, A., Helfter, C., Nemitz, E., O'Doherty, S. J., Palmer, P. I., Pitt, J. R., Rennick, C., Say, D., Stanley, K. M., Stavert, A. R., Young, D., and Rigby, M.: Atmospheric observations consistent with reported decline in the UK's methane emissions (2013–2020), Atmos. Chem. Phys., 21, 16257–16276, https://doi.org/10.5194/acp-21-16257-2021, 2021.

Manning, A. J., Redington, A. L., Say, D., O'Doherty, S., Young, D., Simmonds, P. G., Vollmer, M. K., Mühle, J., Arduini, J., Spain, G., Wisher, A., Maione, M., Schuck, T. J., Stanley, K., Reimann, S., Engel, A., Krummel, P. B., Fraser, P. J., Harth, C. M., Salameh, P. K., Weiss, R. F., Gluckman, R., Brown, P. N., Watterson, J. D., and Arnold, T.: Evidence of a recent decline in UK emissions of hydrofluorocarbons determined by the InTEM inverse model and atmospheric measurements, Atmos. Chem. Phys., 21, 12739‑12755, doi: 10.5194/acp-21-12739-2021, 2021.

Redington, A. L., Manning, A. J., Henne, S., Graziosi, F., Western, L. M., Arduini, J., Ganesan, A. L., Harth, C. M., Maione, M., Mühle, J., O'Doherty, S., Pitt, J., Reimann, S., Rigby, M., Salameh, P. K., Simmonds, P. G., Spain, T. G., Stanley, K., Vollmer, M. K., Weiss, R. F., and Young, D.: Western European emission estimates of CFC-11, CFC-12 and CCl4 derived from atmospheric measurements from 2008 to 2021, Atmos. Chem. Phys., 23, 7383‑7398, doi: 10.5194/acp-23-7383-2023, 2023.

5. History of the document

Version	Author(s)	Date	Changes
1.0	Stephan Henne EMPA, Anita Ganesan UNIVBRIS, Alistair Manning MO, Tim Arnold (UNIEDIN)	2026-02-13	First draft
1.1	Stephan Henne EMPA, Anita Ganesan UNIVBRIS, Alistair Manning MO, Tim Arnold (UNIEDIN)	2026-02-19	Second draft